

A novel technique for dressing metal-bonded diamond grinding wheel with abrasive waterjet and touch truing

Zhenzhong Zhang¹ · Peng Yao¹ · Zhiyu Zhang² · Donglin Xue² · Chong Wang¹ · Chuanzhen Huang¹ · Hongtao Zhu¹

Received: 24 February 2017 / Accepted: 26 June 2017 / Published online: 12 July 2017
© Springer-Verlag London Ltd. 2017

Abstract The dressing of metal-bonded diamond grinding wheels is difficult despite their availabilities on hard and brittle materials. In this paper, a novel compound technology that combines abrasive waterjet (AWJ) and touch truing is proposed for dressing metal-bonded diamond grinding wheel precisely and efficiently. The dressing experiments of a coarse-grained and a fine-grained bronze-bonded diamond grinding wheel were carried out on a surface grinder with a developed AWJ system. The feasibility of this method was verified by analyzing the wheel runout, the truing forces, and the wheel surface topography. The variations of 3D surface roughness of wheel surface topography during the compound dressing process were quantitatively analyzed. The mechanism of AWJ and touch compound dressing is also discussed. Further, a reaction-bonded silicon carbide block was ground to validate the dressing quality. The experiment results indicate that the grinding wheels that were well dressed by the proposed technique leads to a smaller grinding force and a smaller surface roughness than that of undressed wheels.

Keywords Dressing · Abrasive waterjet · Touch truing · Diamond grinding wheel · 3D surface roughness

1 Introduction

Hard and brittle materials are extensively utilized in advanced industrial technologies, especially in optics. Reaction-bonded silicon carbide (RB-SiC) is one of the typical materials. Superabrasive grinding wheels have superior performances such as long wheel life, high precision and high efficiency, which is regarded as the most efficient tools to machine these hard and brittle materials [1]. Dressing of the grinding wheel needs to be conducted to make certain of the precise geometry and sharpness. However, the difficulty of dressing process is greatly increased due to excellent wearability of superabrasive grinding wheel, especially a sintered metal-bonded superabrasive wheel with a large circular runout and low grit protrusion height. In order to solve these problems, many alternate high-efficiency and high-precision dressing techniques have been developed recently.

Touch dressing was used primarily for monolayer bonded grinding wheels. At present, it is also developed for other bonding systems to improve the effective roughness of the grinding wheel and to reduce the runout, it enables participation of large number of inactive grits before the dressing [2], which not only reduces the ground surface roughness greatly but also maintains an almost constant roughness value over a long span of grinding [3]. There are two major types of touch dressing tools, including dressing blocks and rotary-powered rollers [4]. Yegenoglu and Roth [5] first applied touch dressing in grinding of cast iron with a monolayer electroplated CBN wheel and brazed CBN wheel. Ghosh and Chattopadhyay [6] investigated the feasibility of the touch dressing with brazed CBN with different grain distributions.

✉ Peng Yao
yaopeng@sdu.edu.cn

Zhiyu Zhang
zhangzhiyu@ciomp.ac.cn

¹ Center for Advanced Jet Engineering Technologies (CaJET), Key Laboratory of High-efficiency and Clean Mechanical Manufacture (Ministry of Education), School of Mechanical Engineering, Shandong University, Jingshi Road 17923, Jinan 250061, China

² Key Laboratory of Optical System Advanced Manufacturing Technology, Changchun Institute of Optics, Fine Mechanics and Physics, Chinese Academy of Sciences, Changchun 130033, China

The brazed CBN wheels were dressed by touch dressing so that abrasive cutting edges get micro-trued and allow the next layer grits to involve in grinding and thus improve the grinding quality. Su et al. [7] proposed a new method for touch dressing diamond wheel by grinding block composed of soft steel and SiC abrasive, which strongly converts tip atoms of the diamond to iron carbon compounds or graphite through chemical actions. Suzuki et al. [8] proposed a new type of truing method of the diamond wheel by grinding alloyed metals. Their results showed that truing efficiency and accuracy were increased greatly by utilizing alloy metals (Mo, Nb, and Ta). The reason is that they react with the carbon atom of diamond. The chip pockets of the diamond grinding wheel will be reduced after touch dressing, which may lead to great increasing of the grinding force and the grinding heat. And then it affects the quality of the grinding, the form accuracy is decreased and the depth of subsurface damage is increased. Moreover, the abrasive grains will become blunt and the service life of the grinding wheel will be reduced due to rigid contact.

Abrasive waterjet (AWJ) is a recently developed high-efficiency machining technology, which causes no mechanical damage of grains and tool wear [9]. Jurisevic et al. [10] compared this technology with other traditional processing methods, little or no thermal effect is favorable to keep the work piece undeformed. Meanwhile, some advantages of AWJ including wide processing range, high-kerf quality, ability to cut free form surface at close tolerances effectively, easy achievement of diverse cutting patterns under computer control, etc. are making it ideal for on-machine and in-process dressing. Therefore, this is a promising tool for conditioning of the wheel by abrasive waterjet, and researchers have done some attempt study for the abrasive waterjet dressing of wheels. Hirao et al. [11] offered a proposal of using high-pressure waterjet to remove chips from the metal-bonded CBN wheel without damaging the wheel. Shen et al. [12] applied waterjet to dress metal bond diamond wheel for lap grinding of Al_2O_3 ceramics. The experimental results show that the metal bond diamond wheel can be well dressed with waterjet by which the efficiency of precision machining can be improved. Axinte et al. [13] reported on a specific application of AWJ turning, i.e., truing and dressing of Al_2O_3 grinding wheels. The results of the experiment demonstrated that abrasive waterjet turning integrates the kinematics of a conventional turning process with the advantages of abrasive waterjet cutting. It will remove abrasive grits as well as binder on the circumference of the grinding wheel progressively. The removal rate of the high point is higher than that of the low point in grinding wheel, so as to achieve reducing circle runout error of grinding wheels. The results also showed that the accuracy of the trued wheel profile decreases as the stand-off distance increasing. Tolerance for achieved primitive profiles is almost ± 0.01 mm. Li et al. [14] pointed out that when

the gap between the grinding wheel and a workpiece is very small, the speed and energy of slurry jet which aims at the gap were enhanced to improve the impact capacity greatly. Yao et al. [15] investigated the effect of AWJ dressing of resinoid-bonded diamond wheels and concluded that the dressing effect of abrasive waterjet is superior to waterjet. The protrusion height of the diamond grits becomes distinct and the abrasive grains distribute uniformly on the wheel surface after dressing with abrasive waterjet.

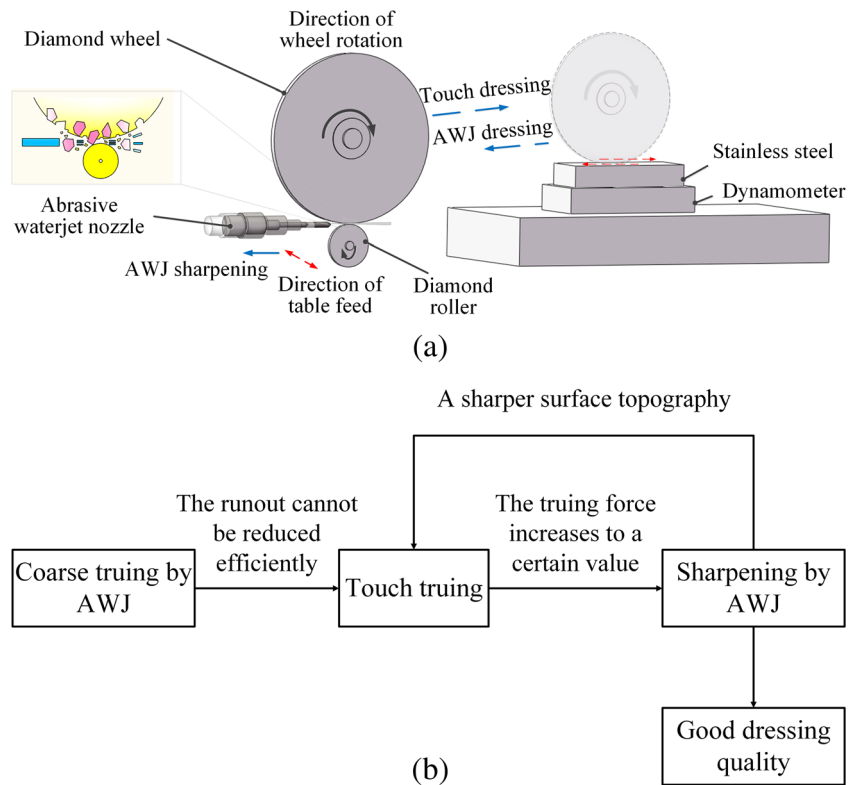
The grains of a metal-bonded diamond wheel randomly distribute in the iron or bronze bond. The chief purposes in the AWJ dressing metal-bonded diamond wheels are to realize the removal of the bond materials effectively without damaging or breaking the diamond grains, and a good protrusion of grains is obtained. It was found that the mode of material removal is due to fracture and scratching of reinforcement particles in metal matrix composites (MMC) and ductile fracture of matrix material in machining Al-SiC particulate metal matrix composites by AWJ [16]. Pramanik [17] noted the removal rate of reinforcement material is much slower than that of matrix material due to its high stiffness when reinforcement particles in metal matrix composites are very large compared with abrasive particles in the waterjet. The procedure produces uniform protrusions of reinforcement particles on the matrix material surface. However, the removal mechanism of the AWJ dressing of metal-bonded diamond wheels has not yet been covered.

In this paper, a novel dressing method, namely compound dressing with abrasive waterjet and grinding, is proposed to take advantages of conventional touch dressing and abrasive waterjet dressing. To prove the feasibility of this new method, an experimental study was conducted by comparing the output of dressing such as radial runout, truing forces, force ratios, and wheel topographies after truing and sharpening. The material removal mechanisms in the AWJ and touch compound dressing of diamond grinding wheel were discussed. The new dressing method not only achieves high truing efficiency and dressing quality, but also ensures a small grinding force of the whole process to protect the spindle and slide of machine tool.

2 Principles and procedures of dressing with AWJ and touch truing

The schematic of compound dressing is shown in Fig. 1a and b. The dressing process is divided into three steps, it includes the abrasive waterjet coarse truing, touch fine truing, and abrasive waterjet sharpening. The first two steps aim at decreasing the grinding wheel geometric deviation efficiently. The purpose of the third step is to increase the protrusion height of the abrasive grains on the wheel working surface.

Fig. 1 Schematic diagram of dressing by AWJ and touch truing
a The principle of dressing **b** The process of dressing



- (1) The high-efficient coarse truing by abrasive waterjet under the constraint of diamond roller: During this operation, abrasive waterjet turning is applied to profile grinding wheel. The superabrasive grinding wheel and electroplated diamond roller are kept away from each other with a gap of $1/4 \sim 1/2$ of abrasive particle size. The grinding wheel reciprocates along the axial direction. The abrasive waterjet dressing head was installed on the grinder along the tangential direction of the grinding wheel and aiming at the gap. Under the constraint of the diamond roller surface, the high-pressure waterjet stream is focused and sprayed from the abrasive waterjet nozzle to the target superabrasive grinding wheel in a tangential mode at a stand-off distance.
- (2) Touch truing by grinding stainless steel: Due to the limitation of the machining accuracy of abrasive waterjet, the runout cannot be reduced efficiently when the wheel runout is reduced to a certain value. A stainless steel (SUS304) block is ground by the superabrasive grinding wheel trued after step 1 to achieve fine truing, then the abrasive grains protruding from bond can be machined to uniform protrusion height.
- (3) Sharpening by abrasive waterjet: With the increment of wheel wear, the truing force increases during touch truing. In order to reduce truing force and obtain an ideal wheel surface topography with abrasive cutting edges

protruding from the bond material and providing adequate chip pockets, the abrasive waterjet with low pressure and large stand-off distance is adopted to improve the protrusion height of diamond grains. Then, the alternation of two steps is chosen to speed up the diamond wear rate to dress the grinding wheel.

3 Experimental setup

The dressing experiments were conducted on an ultra-precision surface grinding machine NAS520 CNC with an AWJ system. The experiment setup is illustrated in Fig. 2a. As shown in Fig. 2b, the abrasive waterjet dressing head was fixed on the grinding machine and the nozzle was set along the tangential direction of the grinding wheel and gap between grinding wheel and diamond roller. The high-velocity abrasive waterjet was focused and ejected to the target superabrasive grinding wheel from the abrasive waterjet nozzle in a tangential mode at a stand-off distance. The abrasive flow rate can be adjusted by a control valve installed in the abrasive pipe. Some protective measures have been taken to avoid the damage of AWJ on the machine. For example, protecting covers are installed to prevent the wear of slides, spindle, and other part of the machine, and a new channel is provided for collecting used abrasives and water to avoid them

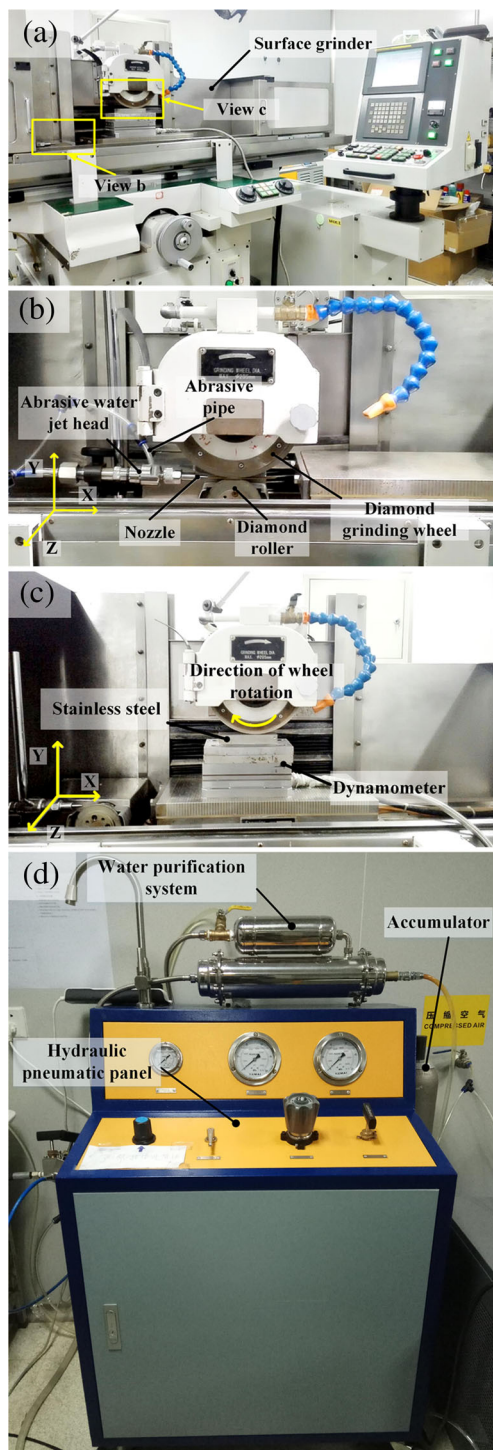


Fig. 2 Setup for conditioning experiments. **a** Global structure. **b** Partial structure from view b. **c** Partial structure from view c. **d** Pneumatic fluid pressurization system force was measured by a three-component force dynamometer (Kistler, Model 9257B) fasten under the stainless block. High-pressure water is supplied by the pneumatic fluid pressurization system as shown in Fig. 2d. The maximum pressure and flow rate of the system are 10,000 PSI and 5 L/min, respectively

flowing into the coolant tank and mixing with the coolant during the AWJ dressing process.

A stainless steel (SUS304) block was chosen to speed up wheel wear rate and improve the efficiency of truing. During the compound dressing process of diamond wheel, as shown in Fig. 2c, the truing.

Two bronze-bonded diamond grinding wheels with different grain sizes were dressed in the experiments. The diameter and width of the grinding wheel were 200 mm and 8 mm, respectively. The grinding wheel was dressed by electric discharge machining (EDM) before delivery. The initial runout of the grinding wheel was around 100 μm . Before dressing, the dynamic balance of the grinding wheel was adjusted to retain a low-wheel vibration amplitude under 0.03 μm during grinding. The dressing conditions are listed in Table 1.

Wheel radial runout before and after dressing is measured by a laser displacement sensor (Keyence LK-G10). In order to obtain the topographies of wheel surface before and after the compound dressing, the variation of wheel surface on a removable wheel block was observed by a 3D laser scanning confocal microscope (Keyence VK-X200K).

A RB-SiC block was ground to compare the performance of the grinding wheel before and after dressing. The work piece was clamped on the three-component force dynamometer and fixed on the table of the surface grinder. It was ground with a depth of cut of 2 μm , a peripheral speed of 20 m/s, and a table speed of 13,600 mm/min. The average surface roughness (R_a) of the workpiece was measured at five different positions on the surface by a portable surface roughness tester. The measuring direction is vertical to the feed direction of table.

4 Result and discussions

4.1 Truing accuracy

Truing accuracy is crucial for making the AWJ and touch compound dressing feasible. Wheel radial runout is often used to characterize the truing accuracy. The wheel runout with grain size #120 and #1500 under three different conditions are indicated in Fig. 3. As shown in Fig. 3a and d, both the roundness error and the eccentricity of the new wheels lead to the large runouts of 103 μm and 49 μm , respectively. The eccentricity is the primary cause of the large wheel runout, which needs to be trued. Figure 4 shows the variation of wheel radial runout of the three steps under given conditions. The removal rate of #120 wheel is high at the beginning of the dressing process. However, because of the limitation of the truing accuracy of abrasive waterjet, the runout cannot be reduced efficiently when it is smaller than 60 μm as shown in Fig. 4. The radar map of grinding wheel runout after coarse truing is shown in Fig. 3b and e. The wheel should be further dressed to reduce the eccentricity and the roundness error. The decrement rate of the wheel radial runout at the initial AWJ truing stage is greater than those in touch truing. As shown in

Table 1 The dressing conditions

Dressing condition	
Wheel characteristics	
Grain	Diamond
Grit size	#120 (105 to 125 μm) #1500 (7 to 10 μm)
Bond	Bronze
AWJ characteristics	
Abrasive material	Garnet
Orifice diameter	0.25 mm
Nozzle diameter	0.76 mm
Coarse truing parameters	
Abrasive in waterjet	150# (75 to 106 μm)
Jet pressure	40 MPa
Stand-off	15 mm
Abrasive flowrate	12 g/min
Wheel speed	5 m/s
Roller speed	10 m/s
Wheel axial feed speed	400 mm/min
Fine truing parameters	
Wheel speed	10 m/s
Feed rate of worktable	3400 mm/min
Grinding depth	10 $\mu\text{m}/5 \mu\text{m}$
Sharpening parameters	
Abrasive in waterjet	#150 (74 to 105 μm)
Jet pressure	30 MPa
Stand-off	20 mm
Abrasive flowrate	9 g/min
Wheel speed	5 m/s
Wheel axial feed speed	400 mm/min

Fig. 4, the two kinds of dressing method are conducted alternatively to speed up the diamond wear rate and ensure a small truing force. As indicated in Fig. 3c and f, the runout error of the #120 wheel and the #1500 wheel were reduced to 12.9 μm and 1.1 μm at last, respectively. It is obvious that the dressing efficiency of the #1500 grinding wheel was much higher than that of the #120 grinding wheel. Therefore, the grinding wheel with small grains can be trued more precisely and efficiently by the proposed compound dressing technique.

4.2 Truing force

The truing forces of the first touch truing step for the two grinding wheels are shown in Fig. 5. The normal truing forces of both #120 wheel and #1500 wheel increase with time significantly compared to tangential truing forces. This is mainly resulted from the grains worn out and the chips stuck to the wheel in touch truing. The ascent rate of truing force of #1500 wheel is much larger than that of #120 wheel because of the

higher wear rate of the fine-grained grinding wheels. The great forces are unfavorable to the dressing of the grinding wheel. Figure 6 shows the variation of truing forces of in the normal and tangential directions before and after AWJ sharpening. It can be seen that the truing force in the two directions after AWJ sharpening is much smaller than those of before AWJ sharpening. The smaller forces will help to protect the machine tool spindle system and improve grinding wheel profile accuracy.

The force ratio F_n/F_t in a grinding process is a characteristic value of sharpness of a grinding wheel. Low force ratio means that the wheel is well-dressed, and grits have sharp cutting edge to remove workpiece material. The ratios of the normal force to the tangential force in this experiment are shown in Fig. 6. The ratios in touch truing after AWJ sharpening are smaller than that before case, which indicate greater sharpness of abrasive grains in the coarse and fine grinding wheels surface after AWJ sharpening.

4.3 Evaluation of dressed wheel surface

4.3.1 Wheel topography before and after dressing

The micrographs of surface topography of the #120 wheel and #1500 wheel are indicated in Fig. 7. Figure 7a and e indicates the surface topography of the diamond wheel before dressing. Most of the diamond grits on the surface of the new diamond grinding wheel are embedded in the binder, and the binder melts to the heat effect superficial layer in the thermal removal process caused by EDM dressing before delivery. Figure 7b and f indicates the surface topography of the diamond wheel after coarse truing by AWJ. Due to the effect of the large AWJ impact load caused by high pressure and the small stand-off distance, not only the metal bond material was removed quickly but also the diamond grains were pulled out from the binder. Consequently, the number of grains on diamond wheel surface reduced greatly. Figure 7c and g indicates the surface topographies of the two diamond wheels after the first touch truing. Most of the grains on the surface became flattened or chipped due to the shear and extrusion force in the traditional touch truing. There are some pits on the grinding wheel surface because of some diamond grains falling off from the binder. Therefore, the protrusion height of grains obviously decreased, and the grinding performance is reduced or even lost. Figure 7d and h indicates the surface topographies of the two diamond wheels after the last AWJ sharpening process, where many angular diamond abrasives stick out of the wheel surface. The metal bond material among abrasive grains was removed with rarely affecting grains under the smaller AWJ impact load. Hence, the truncated or embedded diamond grains protruded from the bond. Some chip space in the diamond wheel was obtained. The comparison and analysis of observed wheel surface topographies verified that the

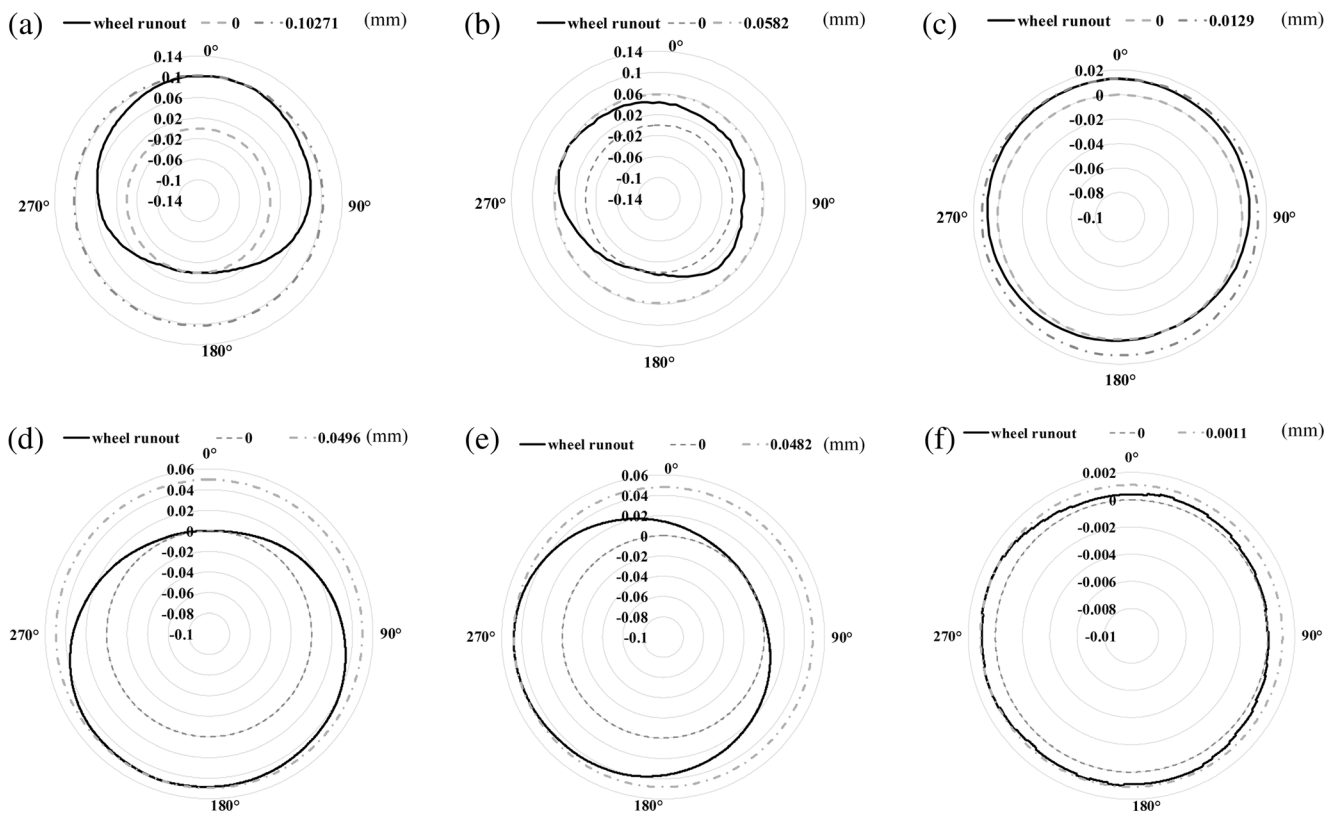


Fig. 3 Radar maps of runout of the #120 and #1500 grinding wheels under different conditions. **a** The new #120 wheel. **b** The #120 wheel after coarse truing by AWJ. **c** The #120 wheel after compound dressing. **d**

The new #1500 wheel. **e** The #1500 wheel after coarse truing by AWJ. **f** The #1500 wheel after compound dressing

bronze-bonded diamond grinding wheel was well-dressed by the novel compound dressing method.

4.3.2 3D amplitude roughness parameters of wheel surface topography before and after dressing

3D amplitude roughness parameters of the grinding wheel surface topography have been investigated in this research.

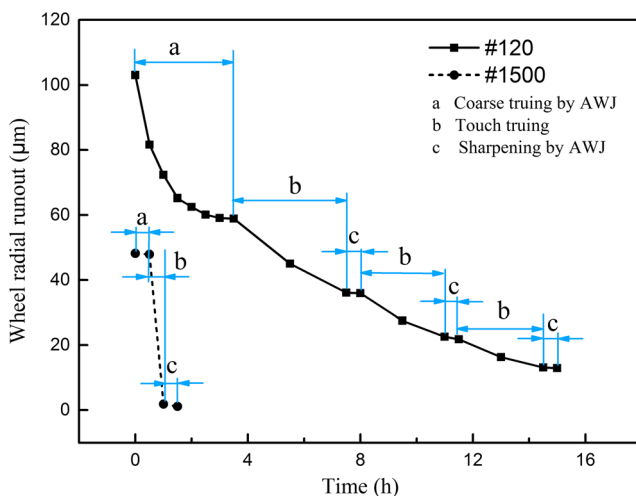


Fig. 4 Radial runouts of #120 and #1500 grinding wheels versus time

The wheel surface characteristics before and after dressing are quantitatively described in terms of 3D amplitude parameters of surface roughness listed in Table 2 [18]. The mathematical expression and the corresponding characteristic of wheel surface of root mean square roughness S_q , the maximum peak height S_p , the skewness S_{sk} , and the

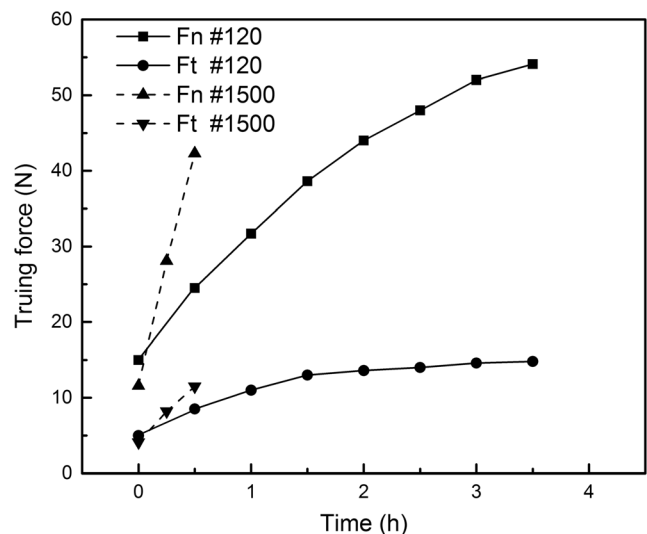
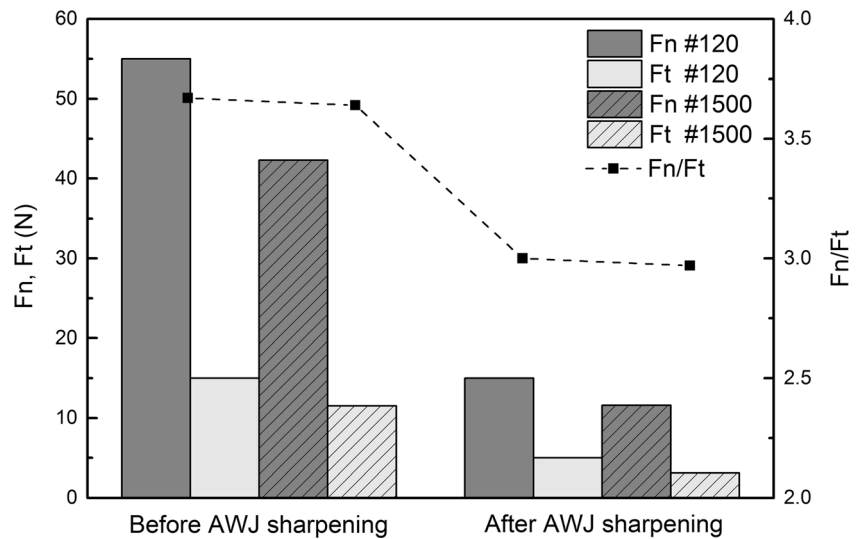


Fig. 5 Truing forces of #120 and #1500 grinding wheels during the first touch truing step

Fig. 6 Touch truing forces (F_t , F_n) and ratios of normal to tangential force (F_n/F_t) of #120 and #1500 wheels before and after AWJ sharpening



kurtosis S_{ku} are explained in this table. The measured parameters are shown in Fig. 8. The 3D amplitude parameters

of the #1500 wheel show same variation trends with those of the #120 wheel.

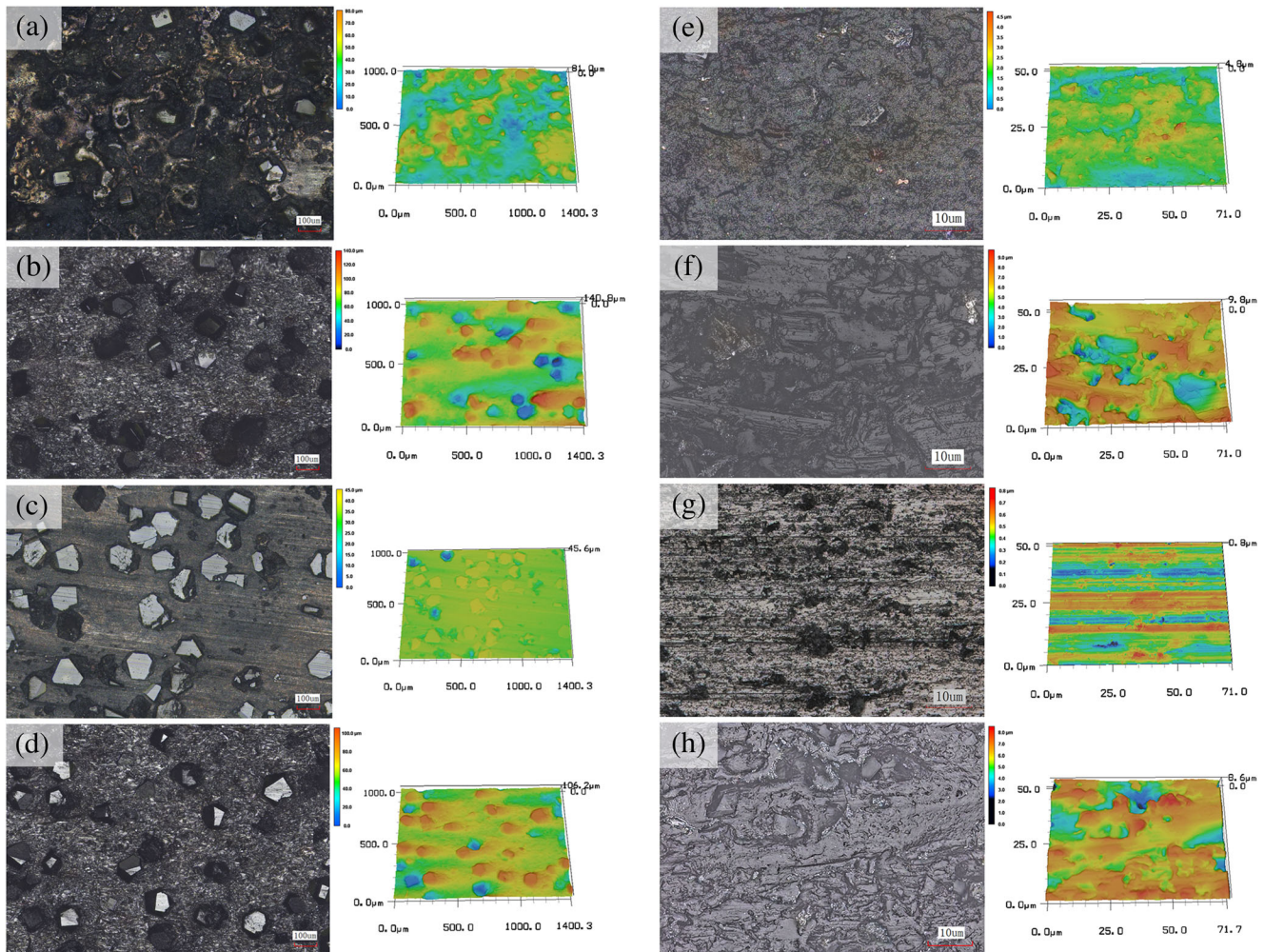


Fig. 7 Surface topographies of #120 and #1500 diamond grinding wheels at different conditions **a** #120 wheel before dressing **b** #120 wheel after coarse truing by AWJ. **c** #120 wheel after touch truing. **d**

#120 wheel after AWJ sharpening **e** #1500 wheel before dressing **f** #1500 wheel after coarse truing by AWJ. **g** #1500 wheel after touch truing. **h** #1500 wheel after AWJ sharpening

Table 2 3D amplitude roughness parameters of grinding wheel surface

Amplitude parameters	Statistical	Characteristic of surface
Root mean square roughness Sq	$Sq = \sqrt{\iint_a (Z(x, y))^2 dx dy}$	Stand for a comprehensive measure of the texture comprising the surface A larger value of Sq means a rougher wheel surface
Maximum peak height Sp	$Sp = \text{Max}[Z(x, y)]$	Maximum protrusion height A larger value of Sp means a larger protrusion height of abrasive grains
Skewness Ssk	$Ssk = \frac{1}{Sq^3} \iint_a (Z(x, y))^3 dx dy$	Measure the profile symmetry about the mean plane Ssk < 0, indicates the wheel surface with predominantly peak-type features Ssk > 0, indicates the wheel surface with predominantly valley-type features
Kurtosis Sku	$Sku = \frac{1}{Sq^4} \iint_a (Z(x, y))^4 dx dy$	Measure the sharpness of the surface height distribution A more centrally distributed height distribution has a larger value of Sku means

Figure 8a illustrates the effect of dressing on the height distribution of surface topography. For example, the RMS roughness Sq of the #120 wheel surface after AWJ truing and AWJ sharpening varies from 12.65 to 13.86 then to 19.58, compared to the initial wheel surface. These trends demonstrate the roughness of the surface after AWJ dressing

increased dramatically. Conversely, the Sq of the wheel surface after touch truing decreased remarkably. The reason for this is that the grinding wheel worn by touch truing, and the protrusion high of abrasive cutting edges was small. The variation of the maximum peak height Sp of the wheel surface is indicated in Fig. 8b. This indicates that the peak height

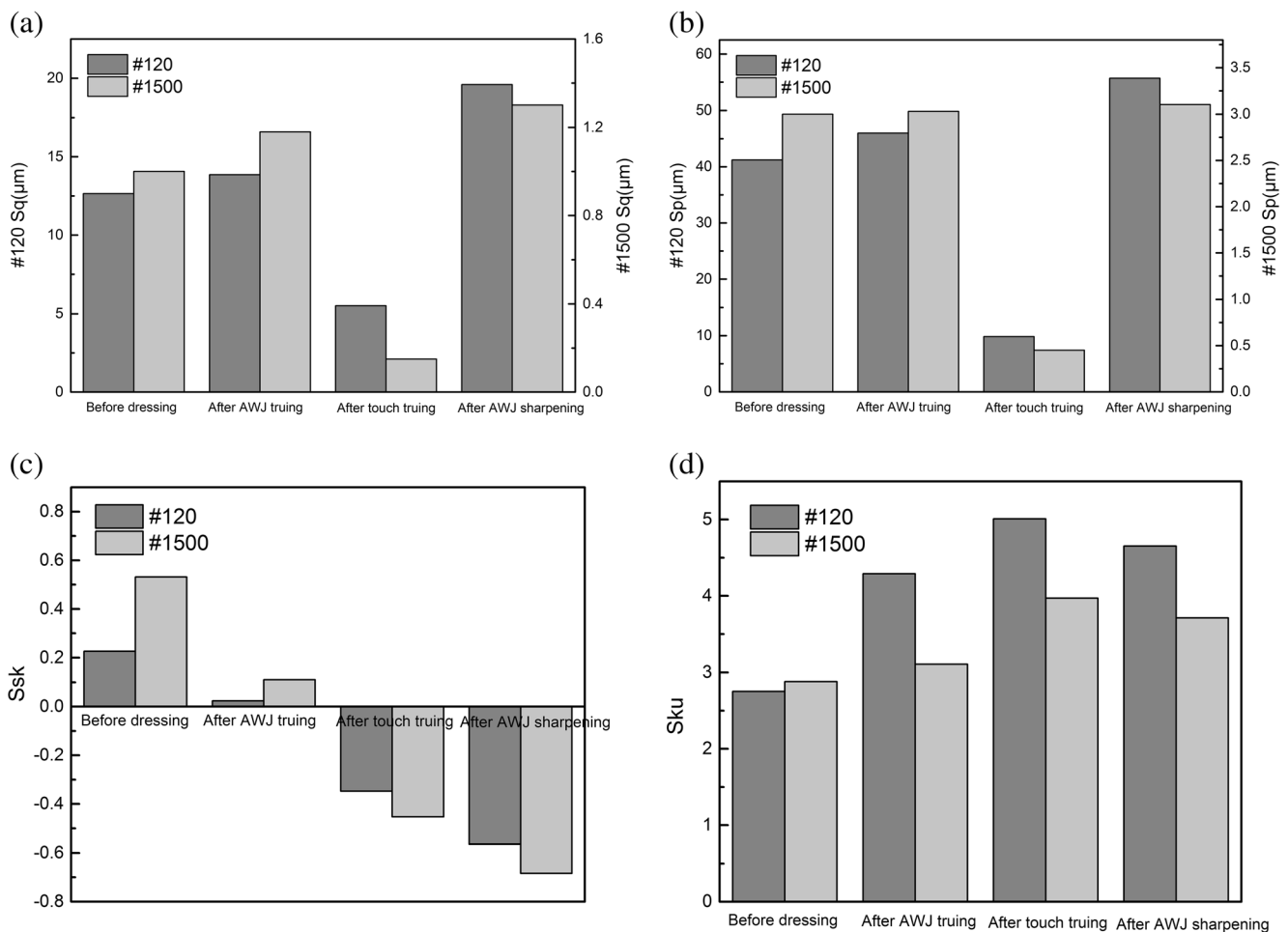


Fig. 8 Amplitude parameters of 3D surface roughness of #120 and #1500 grinding wheels' surface topography before and after dressing. **a** RMS roughness. **b** Maximum peak height. **c** Skewness. **d** Kurtosis

increases dramatically after AWJ dressing, expectedly, because of the generation of the higher protrusion of diamond grain. However, the maximum peak height after touch truing is less than that after the other dressing steps. The variation in height distribution is mainly due to the effective worn out of grain cutting edges through the chemical-mechanical effect between diamond and stainless steel during touch truing. Meanwhile, the grain loss caused by fracture and/or dislodgment of the entire abrasive grain during the touch truing process also lead to the decrease of S_p . The value of S_q and S_p of #1500 wheel are quite smaller than those of the #120 wheel because of its small grain size and protrusion height.

If the surface heights are normally distributed, then S_{sk} is 0.00 and S_{ku} is 3.00. When the $S_{sk} < 0$, it shows the predominance of peaks rather than valley on the surface of diamond wheel. In the Fig. 8c, the S_{sk} of #120 and #1500 wheel surface decreased with the proceeding of dressing process, they became negative after touch truing, and the absolute value increased to 0.56 and 0.68 after AWJ sharpening. The decrease of S_{sk} shows the increase of the volume ratio of protruded grains to the valleys caused by the dislodgment of grains. Figure 8d shows that the kurtosis increased obviously after AWJ truing. Large S_q and S_{ku} indicate a good protrusion status of grains on the wheel surface, but a dramatic decrease of S_q and increase of S_{ku} indicates worn out of grinding wheel [19]. Therefore, grains protruded well from binder after AWJ truing and sharpening, but the grinding wheel worn out after touch truing. The results reveal that the surface topography transformed from a blunt surface to a sharper wheel surface after final AWJ sharpening.

4.4 Material removal mechanisms in compound dressing

Figure 9 shows the photographs of the #120 wheel surface as delivered, after touch truing and after AWJ dressing. To reveal

the material removal mechanism of the compound dressing, the grains and binder were observed under a higher magnification. As shown in the left side, it is obvious that the diamond tips wear flat after touch truing, the extrusion force during grinding stainless steel could cause the micro-cracks on the grits, some diamond grits are pulled out during grinding. This is due to the fact that chemical actions convert strongly tip atoms of diamond to iron carbon compounds or graphite, then mechanical action delivers the energy debonding the surface chemical reaction products of the diamond tip. As shown in the right side, the AWJ dressing utilized impingement of solid particles to remove the metal bonds. It can be seen from the figure that many separated wear tracks were scratched and plowed on the binder by high-speed single abrasive grains. Moreover, the tracks are longer and shallower and do show a uniform orientation, preferably in the jet direction. Some voids are generated by the dislodgement of diamond abrasives from the bonding material during AWJ dressing. Therefore, in the erosion of the grinding wheel caused by impacting of high-speed solid particles, there are three major mechanisms such as micro-cutting of binder, brittle fracture, and dislodgement of grains. The schematics in Fig. 9 illustrate that the material removal of the wheel surface, as the jet moves forward into the material, micro-cutting is the dominating material-removal process due to small impact angle. The grit plowed a groove via plastic deformation of the binder, left a ductile-ground groove, and a subsurface region of plastically deformed material. Gradually, diamond grits were protruded from the wheel surface.

4.5 Workpiece surface ground by new diamond wheel and compound dressed diamond wheel

To verify the effectiveness of this new compound dressing method, the wheel performance during grinding is analyzed. The comparison grinding experiments were carried out on

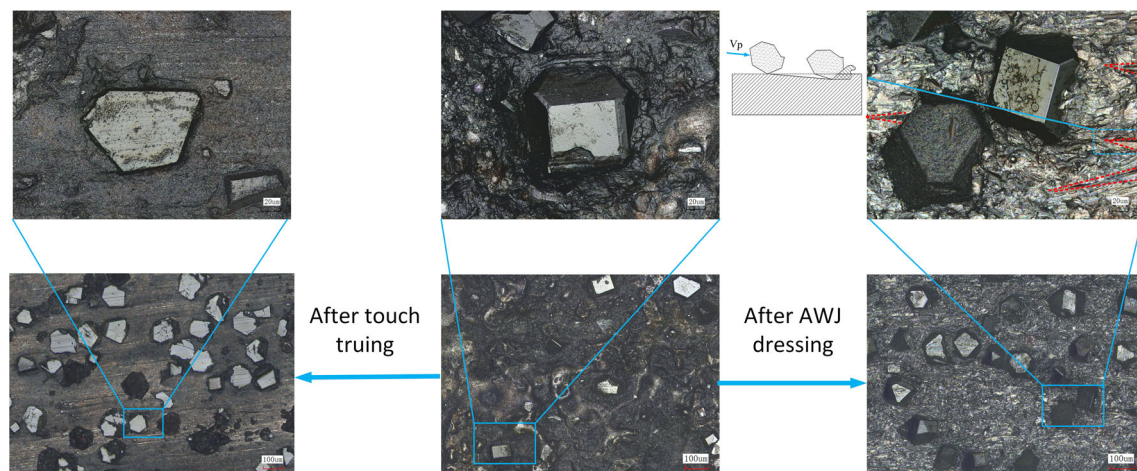


Fig. 9 Material removal mechanism in compound dressing

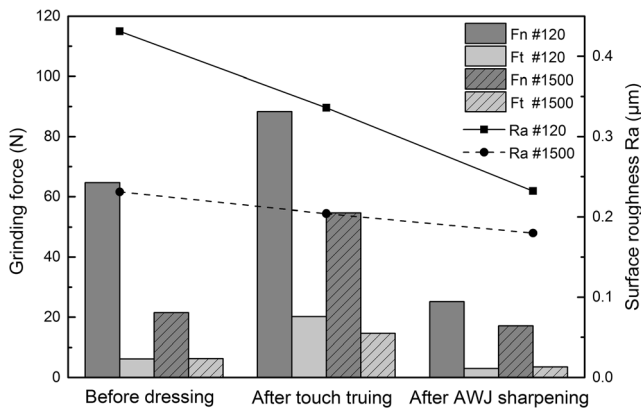


Fig. 10 Grinding forces (Fn, Ft) and surface roughness Ra at different wheel conditions for #120 and #1500 wheels

RB-SiC workpiece with the two diamond wheels under three different conditions including before dressing, after touch truing and after AWJ sharpening. Figure 10 shows the values of normal grinding force Fn, tangential grinding force Ft, and surface roughness of ground workpiece at different conditions for the two wheels. The grind force and surface roughness gained by the #1500 wheel and the #120 wheel show same variation trends.

The lowest grinding forces and the smallest surface roughness can be obtained after AWJ sharpening. Compared with the new wheel, it can be found that a reduction in surface roughness can be obtained by grinding with the two diamond wheels after touch truing and AWJ sharpening, which does indicate the increase of effective grains number and more uniform protrusion height of grains in grinding. The grinding forces after touch truing were larger than that of new grinding wheel, which indicates the decrease of grain protrusion and the increase of blunt grains on the wheel surface. Therefore, the following AWJ sharpening is necessary to decrease the grinding force.

5 Conclusions

A novel compound dressing method with AWJ and touch truing was proposed and applied to dress a metal-bonded diamond grinding wheel. By utilizing the merits of conventional touch dressing methods and abrasive waterjet dressing methods, both high truing efficiency and good dressing quality are achieved.

- (1) The variations of wheel radial runout during the compound dressing show that the fine-grained grinding wheel can be trued more precisely and more efficiently than that of coarse-grained grinding wheel.
- (2) The truing force and the force ratio after AWJ sharpening were much smaller than that in touch truing, which

indicate the increased sharpness of wheel surface after AWJ sharpening.

- (3) Observation and quantitative assessment of the grinding wheel topography after different dressing steps indicate that the grains on the surface of the coarse and fine-grained grinding wheels protruded well from binder after AWJ truing and sharpening, but the grinding wheel worn out rapidly after touch truing.
- (4) Micro observation of AWJ and touch-dressed wheel surface topographies show that the removal mechanism of material in AWJ dressing is micro-cutting of binder, brittle fracture, and dislodgement of grains.
- (5) The surface grinding experiment results of RB-SiC show that the compound dressing method with AWJ and touch truing can improve wheel performance and ground surface quality.

Acknowledgements This work is supported by National Science and Technology Major Project (Grant No. 2015ZX04003006), Key Laboratory of Optical System Advanced Manufacturing Technology (Grant No. Y4GX1SJ141) and Key Laboratory for Precision and Non-traditional Machining of Ministry of Education, Dalian University of Technology (Grant No. JMTZ201504).

References

1. Wang Y, Zhou XJ, Hu DJ (2006) An experimental investigation of dry-electrical discharge assisted truing and dressing of metal bonded diamond wheel. *Int J Mach Tools Manuf* 46:333–342. doi:10.1016/j.ijmachtools.2005.05.022
2. Wegener K, Hoffmeister HW, Karpuschewski B, Kuster F, Hahmann WC, Rabiey M (2011) Conditioning and monitoring of grinding wheels. *CIRP Ann Manuf Technol* 60:757–777. doi:10.1016/j.cirp.2011.05.003
3. Wenfeng D, Linke B, Zheng Y, Yucan J (2016) Review on monolayer CBN superabrasive wheels for grinding metallic materials. *Chin J Aeronaut* 30:109–134. doi:10.1016/j.cja.2016.07.003
4. Guo B, Zhao Q (2014) Mechanical truing of v-shape diamond wheels for micro-structured surface grinding. *Int J Adv Manuf Technol* 78:1067–1073. doi:10.1007/s00170-014-6721-7
5. Yegenoglu K, Roth M (1987) Good surface finish with electroplated CBN wheels. *Ind Diam Rev* 47:114–116
6. Ghosh A, Chattopadhyay AK (2007) Experimental investigation on performance of touch-dressed single-layer brazed CBN wheels. *Int J Mach Tools Manuf* 47:1206–1213. doi:10.1016/j.ijmachtools.2006.08.020
7. Su HH, Xu JH, Fu YC, Ding WF, Wang S (2011) Experimental study on performance of monolayer brazed diamond wheel through chemical-mechanical dressing. *Adv Mater Res* 325:208–212. doi:10.4028/www.scientific.net/AMR.325.208
8. Suzuki H, Okada M, Yamagata Y, Morita S, Higuchi T (2012) Precision grinding of structured ceramic molds by diamond wheel trued with alloy metal. *CIRP Ann Manuf Technol* 61:283–286. doi:10.1016/j.cirp.2012.03.063
9. Li W, Zhu H, Wang J, Ali YM, Huang C (2013) An investigation into the radial-mode abrasive waterjet turning process on high tensile steels. *Int J Mech Sci* 77:365–376. doi:10.1016/j.jmecsci.2013.05.005

10. Jurisevic B, Brissaud D, Junkar M (2004) Monitoring of abrasive water jet (AWJ) cutting using sound detection. *Int J Adv Manuf Technol* 24:733–737. doi:[10.1007/s00170-003-1752-5](https://doi.org/10.1007/s00170-003-1752-5)
11. Hirao M, Izawa M, Iguchi N, Shirase K, Yasui T (1998) Waterjet in-process dressing (1st report). *J Jpn Soc Precis Eng* 64:1335–1339. doi:[10.2493/jjspe.64.1335](https://doi.org/10.2493/jjspe.64.1335)
12. Shen JY, Xu XP, Lin B, Xu YS (2001) Lap-grinding of Al₂O₃ ceramics assisted by water-jet dressing metal bond diamond wheel. *Key Eng Mater* 202–203:171–176. doi:[10.4028/www.scientific.net/KEM.202-203.171](https://doi.org/10.4028/www.scientific.net/KEM.202-203.171)
13. Axinte DA, Stepanian JP, Kong MC, McGourlay J (2009) Abrasive waterjet turning—an efficient method to profile and dress grinding wheels. *Int J Mach Tools Manuf* 49:351–356. doi:[10.1016/j.ijmachtools.2008.11.006](https://doi.org/10.1016/j.ijmachtools.2008.11.006)
14. Li CH, Cai GQ, Xiu SC (2006) Study on surface topography and tribological characteristics finished by abrasive jet with grinding wheel as restraint. *Mater Sci Forum* 532–533:61–64. doi:[10.4028/www.scientific.net/MSF.532-533.61](https://doi.org/10.4028/www.scientific.net/MSF.532-533.61)
15. Yao P, Wei W, Huang CZ, Wang J, Zhu HT, Zhang ZY (2014) High efficiency abrasive waterjet dressing of diamond grinding wheel. *Adv Mater Res* 1017:243–248. doi:[10.4028/www.scientific.net/AMR.1017.243](https://doi.org/10.4028/www.scientific.net/AMR.1017.243)
16. Pramanik A (2014) Developments in the non-traditional machining of particle reinforced metal matrix composites. *Int J Mach Tools Manuf* 86:44–61. doi:[10.1016/j.ijmachtools.2014.07.003](https://doi.org/10.1016/j.ijmachtools.2014.07.003)
17. Srinivas S, Babu NR (2011) Role of garnet and silicon carbide abrasives in abrasive waterjet cutting of aluminum-silicon carbide particulate metal matrix composites. *Int J Appl Res Mech* 1:109–122 http://interscience.in/IJARME_Vol1Iss1/paper22.Pdf
18. Wang W, Yao P, Li C, Huang C, Wang J, Zhu H, Liu Z Dressing of diamond grinding wheels by abrasive water jet for freeform optical surface grinding. In: 7th international symposium on advanced optical manufacturing and testing technologies Harbin China. DOI: [10.1117/12.2068566](https://doi.org/10.1117/12.2068566)
19. Yao P, Gong Y, Matsuda T, Zhou T, Yan J, Kuriyagawa T (2012) Investigation of wheel wear mechanisms during grinding optical glasses through statistical analysis of wheel topography. *Int J Abras Technol* 5:33–47. doi:[10.1504/IJAT.2012.046818](https://doi.org/10.1504/IJAT.2012.046818)